**A novel RHH family transcription factor aCcr1 and its viral homologs dictate cell cycle progression in archaea**

Yunfeng Yang[1], Junfeng Liu[1, 2 #], Xiaofei Fu[1], Fan Zhou[1], Shuo Zhang[1], Xuemei Zhang[1], Qihong Huang[1], Mart Krupovic[2], Qunxin She[1], Jinfeng Ni[1], Yulong Shen[1 #]

[1] CRISPR and Archaea Biology Research Centre, Microbial Technology Institute and State Key Laboratory of Microbial Technology, Shandong University, Qingdao, P. R. China

[2] Institut Pasteur, Université Paris Cité, CNRS UMR6047, Archaeal Virology Unit, Paris, France.

[#]Correspondence: yulgshen@sdu.edu.cn, julyjunfeng@163.com

## Abstract

Cell cycle regulation is of paramount importance for all forms of life. Here we report that a transcription factor and its viral homologs control cell division in Sulfolobales. The 58-aa-long RHH (ribbon-helix-helix) family protein (designated as aCcr1) is conserved in Crenarchaeota and diverse Sulfolobales viruses. aCcr1 is essential for cell viability of *Saccharolobus islandicus* REY15A (formally *Sulfolobus islandicus* REY15A) and exhibits a cyclic transcription pattern, with the highest level being reached during active cell division (D-phase), subsequent to the expression of CdvA, an archaea-specific cell division protein. Cells over-expressing cellular aCcr1 as well as the homologs encoded by large spindle-shaped viruses *Acidianus* two-tailed virus (ATV) and *Sulfolobus* monocaudavirus 3 (SMV3) show significant growth retardation and cell division failure, manifested as enlarged cells with multiple chromosomes. aCcr1 over-expression results in downregulation of over a dozen of genes including the *cdvA* gene. A conserved motif, aCcr1-box, located between the TATA-binding box and the translation initiation site in the promoters of 13 out of the 17 repressed genes, is critical for the aCcr1 binding. The aCcr1-box is present in the promoters of *cdvA* genes across Sulfolobales, suggesting that aCcr1-mediated *cdvA* repression is an evolutionarily conserved mechanism by which archaeal cells dictate cytokinesis progression, whereas their viruses take advantage of this mechanism to manipulate the host cell cycle.

## Introduction

Cell cycle regulation is of fundamental importance for all organisms. In bacteria, cell cycle is usually divided into B (gap), C (replication), and D (growth and cell division) phases (Dewachter et al., 2018). The DNA replication, chromosome segregation, and cell division are tightly coordinated in the bacterial cell cycle, which ensures that one round of replication occurs per division event and division does not jeopardize genomic integrity. It was suggested that the coordination is achieved through either direct interaction between proteins involved in different cell cycle events or indirect coupling to cell size increase or metabolic status (Dewachter et al., 2018)(Westfall and Levin, 2017; Willis and Huang, 2017). Although cell cycle in eukaryotes is far more complex than the bacterial one, its progression is also tightly regulated, involving multiple layers of regulation. Three sets of factors were identified as the key players in the coordination of the eukaryotic cell cycle: (a) a set of cell cycle-regulated proteins including cyclin-dependent kinases (Cdk)-cyclin complexes and related kinases (Evans et al., 1983; Galderisi et al., 2003), (b) various metabolic enzymes and related metabolites, and (c) reactive-oxygen species (ROS) and cellular redox status (Diaz-Moralli et al., 2013). Cyclin-dependent kinases are the engine of sequential progression through the eukaryotic cell cycle. Cyclins bind substrates and target the Cdks to specific subcellular locations. The formation of cyclin-Cdk complex results in Cdk activation. The oscillations of the cyclins are brought about by the fluctuations in cyclin gene expression and degradation by the ubiquitin mediated proteasome pathway (Morgan, 1995).

The mechanism underlying the cell cycle regulation in Archaea, the third domain of life, remains elusive. Two major cell division machineries are present in Archaea. Whereas euryarchaea depend on the FtsZ-based bacterial-like system, most members of the TACK superphylum, including order Sulfolobales, as well as Asgardarchaeota employ the ESCRT-III/Vps4-based cell division machinery (also called Cdv system) (Caspi and Dekker, 2018; Lindas et al., 2008; Samson et al., 2011). In halophilic euryarchaea, a ribbon-helix-helix (RHH) family transcription factor, CdrS, plays a central role in the cell division regulation (Liao et al., 2021a, 2021b). Crenarchaea, in particular, those from the Sulfolobales display eukaryotic-like cell cycle (Bernander, 2000), including a pre-replicative growth period called the G1 phase, the chromosome replication stage (S phase), a second period of cellular growth (G2 phase), and rapid genome segregation and cell division periods, known as the M and D phases, respectively (Lindas and Bernander, 2013). Cyclic gene expression patterns have been observed in the synchronized cultures of *Sulfolobus acidocaldarius* (Lundgren and Bernander, 2007). No bona fide cyclin homolog has been identified in archaea. Although some proteins possess "cyclin box" domains (e.g. transcription factor B) (Dexl et al., 2018), their functioning as genuine cyclins has not been demonstrated. Certain eukaryotic-like serine/threonine kinases, implicated in stress response in Sulfolobales species, such as *Sulfolobus acidocaldarius* and *Saccharolobus islandicus* (formally *Sulfolobus islandicus*) (Hoffmann et al., 2019; Huang et al., 2020; Huang et al., 2019; Huang et al., 2017; Reimann et al., 2012), exhibit cyclic transcription patterns (Lundgren and Bernander, 2007), but their roles in cell cycle control remain to be investigated. Furthermore, Tarrason Risa et al recently reported that degradation of cell division protein ESCRT-III (CdvB) by proteasome drives cell division progression in *Sulfolobus acidocaldarius* (Tarrason Risa et al., 2020). Collectively, these lines of evidence imply that *Sulfolobales* cells have a simpler eukaryotic-like cell cycle regulation system. Therefore, elucidation of the cell cycle regulation in *Sulfolobales* could provide insights into the origin and evolution of the eukaryotic cell cycle regulation.

The archaeal cell cycle is likely to be regulated, at least partly, on the transcriptional level. The archaeal transcription apparatus is a unique mixture of components from both eukaryotes and bacteria (Lemmens et al., 2019; Lewis and Stracker, 2021). Basal transcription machinery required for transcription initiation, elongation and termination is similar to that of eukaryotes and includes TATA-binding protein (TBP), transcription factor B, an RNA-Pol II-like polymerase, termination factors, and other proteins with homologs in eukaryotes (Lemmens et al., 2019; Lewis and Stracker, 2021; Yue et al., 2020). On the other hand, the transcription regulation relies on bacterial-like transcription factors with RHH and helix-turn-helix motifs. Many archaeal transcription factors have been implicated in the regulation of metabolic processes and response to environmental stresses (Lemmens et al., 2019; Sun et al., 2018). Notably, archaea appear to encode fewer transcription factors compared to bacteria, possibly due to more complex regulation through post-translational modifications, such as phosphorylation (Lemmens et al, 2019) and methylation (Chu et al., 2016; Vorontsov et al., 2016).

Global transcriptional analysis of *S. acidocaldarius* genome by ChIP-chip revealed cell cycle specific transcription changes for 165 genes (Lundgren and Bernander, 2007). Among them were several transcription factors and two serine/threonine protein kinases. Functional and mechanistic analysis of the corresponding proteins could help unveiling the cell cycle regulatory circuit in *Sulfolobales.* In this study, we identified a small RHH family transcription factor, named aCcr1 (for archaeal cell cycle regulator 1), which is essential for cell viability and is involved in the control of cell division in *S. islandicus* REY15A. Over-expression of the cellular and viral aCcr1 homologs leads to cell enlargement and growth retardation. Transcriptomic analysis revealed that a number of genes, including *cdvA* and *ePK1*, are strongly downregulated in cells overexpressing aCcr1. Consistently, the purified cellular and viral aCcr1 proteins bind to the promoters of *cdvA* and *ePK1*, encoding ePK1, a eukaryotic-like serine/threonine protein kinase, specifically at a conserved 9-nt motif (Ccr1-box). Our results demonstrate that aCcr1 plays a key role in cell division regulation and imply that it is also involved in the cell cycle manipulation by viruses.

## MATERIALS AND METHODS

**Strains and growth conditions.** *Saccharolobus islandicus* REY15A was grown aerobically at 75°C in STV medium containing mineral salt, 0.2% (w/v) sucrose (S), 0.2% (w/v) tryptone (T), and a mixed vitamin solution (V). *S. islandicus* REY15A(E233S)(Δ*pyrEF*Δ*lacS*), hereafter E233S, was grown in STVU (STV supplemented with 0.01% (w/v) uracil) medium. The medium was adjusted to pH 3.5 with sulfuric acid, as described previously (Deng et al., 2009). SCV medium containing 0.2% (w/v) casamino acid (C) was used for screening and cultivating uracil prototrophic transformants. ATV medium containing 0.2% (w/v) D-arabinose (A) was used for protein expression. Culture plates were prepared using gelrite (0.8% [w/v]) by mixing 2×STV and an equal volume of 1.6% gelrite. The strains constructed and used in this study are listed in the Supplementary information (Table S1).

**Phase contrast and immunofluorescence microscopy.** For microscopy analysis, 5 μl of cell suspension at the indicated time points were examined under a NIKON TI-E inverted fluorescence microscope (Nikon Japan). Immunofluorescence microscopy analysis was carried out as previously described (Liu et al., 2021b). Briefly, *S. islandicus* REY15A cells were collected and pelleted down at 6,000 rpm for 5 min, re-suspended in 300 μl PBS buffer (137 mM NaCl, 2.7 mM KCl, 10 mM $Na_2HPO_4$ $12H_2O$, 2 mM $KH_2PO_4$, pH7.4), and fixed by addition of 700 μl cold absolute ethanol and kept at 4°C for at least 2 h. The fixed cells were washed for 3 times with PBST (PBS plus 0.05% Tween-20) to remove ethanol. Primary antibodies against ESCRT-III (HuaAn Biotechnology Co., Hangzhou, Zhejiang, China) were added with a dilution of 1:1,000 in PBST and incubated at 4 °C overnight. The cells were washed 3 times and then incubated with the goat anti-rabbit secondary antibodies Alexa Fluor® 488 (1:1,000, Thermo Fisher Scientific, USA) for ESCRT-III, and Concanavalin A Alexa Fluor 647 Conjugate (50 μg/ml, Invitrogen™, Thermo Fisher Scientific, USA) for S-layer, and kept at 4 °C for 2-4 h. The localization of

ESCRT-III was observed under a SP8 confocal microscope, and the data were analysed using Leica Application Suite X (LAS X) software (Leica).

**Flow cytometry analysis.** The procedure for the flow cytometry analysis followed the reported method (Liu et al., 2021a, 2021b). Briefly, approximately $3\times10^7$ cells were collected for flow cytometry analysis. Cells were harvested at the indicated time points and fixed with 70% cool ethanol overnight (>12 h). The fixed cells were then pelleted at 2,800 rpm for 20 min. The cells were re-suspended and washed with 1 ml of PBS buffer. Finally, the cells were pelleted again and resuspended in 100 μl of staining buffer containing 50 μg/ml propidium iodide (PI) or SuperGreen. After staining for 30 min, the DNA content was analysed using the ImageStreamX MarkII Quantitative imaging analysis for flow cytometry system (Merck Millipore, Germany), which was calibrated with non-labelled beads with a diameter of 2 μm. The data from at least 20,000 cells were collected for each sample and the data of the single cells were analysed with the IDEAS software.

**Transcriptome analysis.** Strains of Sis/pSeSD and Sis/pSeSD-aCcr1 were cultured in ATV medium under the conditions as described above. For transcriptomic analysis, culture was inoculated with an initial $OD_{600}$ of 0.05. The cells were pelleted at 7,000 rpm for 10 min after 12 h of cultivation when the $OD_{600}$ reached approximately 0.2. The pellet was resuspended in 1 ml PBS buffer. The cells were pelleted again and stored at -80°C. Total RNA was extracted using the Trizol reagent (Ambion, Austin, TX, USA). Total amounts and the integrity of RNA were assessed using the RNA Nano 6000 Assay Kit of the Bioanalyzer 2100 system (Agilent Technologies, CA, USA). Transcriptomic analysis was performed by Novogene (Beijing, China). About 3 μg of high-quality RNA per sample was used for the construction of RNA-Seq libraries. The libraries are sequenced by the Illumina NovaSeq 6000. Clean reads were aligned to the reference genome sequence of *S. islandicus* REY15A (Guo et al., 2011). The resulting data were then analysed by Fragments Per Kilobase of transcript sequence per Million base pairs sequenced (FPKM) analysis to reveal expression levels of all genes in the *S. islandicus* genome. Differential genome expression analysis (over-expression of aCcr1 versus empty vector) was performed using the DEGSeq R package. The resulting P-values were adjusted using the Benjamini and Hochberg' s approach for controlling the false discovery rate padj<0.05 and |log2(foldchange)| > 0 were set as the threshold for significantly differential expression.

**Cell cycle synchronization.** *S. islandicus* REY15A cells were synchronized as previously described (Liu et al., 2021a; Liu et al., 2021b) with slight modifications. Briefly, cells were first grown aerobically at 75°C with shaking (145 rpm) in 30 ml of STV medium. When the $OD_{600}$ reached 0.6-0.8, the cells were transferred into 300 ml STV medium with an initial estimated $OD_{600}$ of 0.05. When the $OD_{600}$ reached 0.15-0.2, acetic acid was added at a final concentration of 6 mM and the cells were blocked at G2 phase of the cell cycle after 6h treatment. Then, the cells were collected by centrifugation at 3,000 *g* for 10 min at room temperature to remove the acetic acid and washed twice with 0.7% (w/v) sucrose. Finally, the cells were resuspended into 300 ml of pre-warmed STV medium and cultivated as above for subsequent analysis.

**Quantitative reverse transcription PCR (RT-qPCR).** Samples from the control and the aCcr1-over-expression strains were collected at indicated time points (same as for the transcriptome analysis). Total RNA was extracted using SparkZol (SparkJade Co., Shandong, China). First-strand cDNAs were synthesized from the total RNA according to the protocol of the First Strand cDNA Synthesis Kit (Accurate Biotechnology Co., Hunan, China) for RT-qPCR. The resulting cDNA preparations were used to evaluate the mRNA levels of the target genes by qPCR using the SYBR Green Premix Pro Taq HS qPCR Kit (Accurate Biotechnology Co., Hunan, China) and the gene specific primers (Table S2). PCR was performed in an CFX96™ (Bio-Rad) with the following steps: denaturing at 95C° for 30s, 40 cycles of 95C° 5s, 60C° 30s. Relative amounts of mRNAs were evaluated using the comparative Ct method with 16S rRNA as the reference.

**Protein purification and chemical cross-linking.** To purify the wild-type aCcr1 (SiRe_0197) and its mutant proteins from *E. coli,* cells harbouring plasmids pET22b-aCcr1-C-His, pET22b-aCcr1-R2A-C-His, pET22b-aCcr1-K7A-C-His, pET22b-aCcr1-R27A-C-His, pET22b-ATV_gp29-C-His, pET22b- SIRV2_gp21-C-His, pET22b-SMV3_gp63-C-His, and pET22b-STIV2_B60-C-His were grown in 2 litres of LB medium at 37°C with shaking until the optical density $OD_{600}$ reached 0.4~0.6, when 1.0 mM IPTG was added into the cultures and the cells were then grown at 37°C for 4 h with shaking. The cells were harvested by centrifugation at 7,000 *g* for 10 min and then resuspended in the lysis buffer A (50 mM Tris-HCl [pH 7.4], 200 mM NaCl, and 5% glycerol). Then, the cells were crushed with an ultrasonic crusher and cell debris was removed by centrifugation at 12,000 *g* for 15 min. The supernatant was incubated at 70°C for 20 min, centrifuged, and then filtered through a membrane filter (0.45 μm). The samples were loaded onto a Ni-NTA agarose column (Invitrogen) pre-equilibrated with buffer A. Finally, the target protein was eluted with buffer A containing 300 mM imidazole. The eluted sample was analysed using a 18% SDS-PAGE gel. The protein samples were concentrated by ultrafiltration using an Amicon Ultra-3KDa concentrator (Millipore). For further purification, size exclusion chromatography was performed using a Superdex 200 increase 10/300 column (GE Healthcare). The protein concentration was determined by the Bradford method using bovine serum albumin as the standard. To assay the oligomeric status, the wild type aCcr1 protein was incubated with increasing concentrations of glutaraldehyde (0.01 to 0.16%) on ice at 4°C for 15 min. The reaction was then stopped by the addition of SDS-PAGE loading buffer, after which the samples were electrophoresed by 20% SDS–PAGE, and the gel was stained with Coomassie blue R-250.

**Western blotting.** Antibodies against TBP, CdvA and ESCRT-III were produced using synthetic specific peptides (amino acids 18-31, SIPNIEYDPDQFPG for TBP (SiRe_1138); 13-25, GQKVKDIYGREFG for CdvA (SiRe_1173); 194-208 IEQSSRVSQSRPAVR for ESCRT-III (SiRe_1174)). Antibody against SisCcr1 (Ccr1 from *Sulfolobus islandicus* REY15A) was produced using purified recombinant proteins purified from *E. coli*. Antibodies against TBP, CdvA and aCcr1 were produced in rabbit, and CdvA in rat. All the antibodies were produced by HuaAn Biotechnology Co. (Hangzhou, Zhejiang, China). For standard

Western blotting analysis, $2\times10^8$ cells (with or without induction) at the indicated times were collected by centrifugation at 5,000 *g* for 10 minutes and resuspended in 20 μl PBS buffer. After the addition of 5 μl 5× loading buffer, the samples were treated at 100 C° for 10 minutes and analysed by SDS-PAGE. The proteins in the PAGE gel were transferred onto a PVDF membrane at 30 mA for 16 h at 4C°. Membranes were blocked with 5 % (w/v) skimmed milk for 2 h at room temperature. The membrane was washed and incubated with a primary antibody and then the secondary anti-rabbit HRP conjugate antibody (TransGen Biotech company, Beijing, China) following the standard protocol. Finally, the membranes were imaged using an Amersham ImageQuant 800 biomolecular imager (Cytiva).

**Electrophoretic mobility shift assay (EMSA).** Substrates used in EMSA experiments were generated by annealing the complementary oligonucleotides with 5' FAM-labelled oligonucleotides (Table S2). The reaction mixture (20 μl) containing 2 nM of the FAM-labelled substrates and different concentrations of aCcr1 or the mutant proteins was incubated at 37C° for 30 min in binding buffer (25 mM Tris–HCl, pH8.0, 25 mM NaCl, 5 mM $MgCl_2$, 10% glycerol, 1 mM dithiothreitol). After the reaction, samples were loaded onto a 10% native PAGE gel buffered with 0.5× Tris–borate–EDTA (TBE) solution. DNA–protein complexes were separated at 200 V for 60 min. The resulting fluorescence was visualized by an Amersham ImageQuant 800 biomolecular imager (Cytiva).

**Phylogenetic analysis.** aCcr1 homologs were collected by PSI-BLAST (2 iterations against the RefSeq database at NCBI; E=1e-05) (Altschul et al., 1997). The collected sequences were then clustered using MMseq2 (Gabler et al., 2020) to 90% identity over 80% of the protein length. Sequences were aligned using MAFFT v7 (Katoh et al., 2019) and the resultant alignment trimmed using trimal (Capella-Gutierrez et al., 2009), with the gap threshold of 0.2. Maximum likelihood phylogenetic analysis was performed using IQ-Tree (Minh et al., 2020), with the best selected amino acid substitution model being LG+I+G4. The branch support was assessed using SH-aLRT (Guindon et al., 2010).

## Results

### The cyclically transcribed gene aCcr1 is essential for cell viability

A previous genome-wide transcriptomic analysis by microarray revealed seven transcription factors which displayed cyclic expression patterns in *Sulfolobus acidocaldarius* (Lundgren and Bernander, 2007). These include one of the three eukaryotic transcription initiation factor IIB homologs, Tfb2 (Saci_1341), an RHH domain protein (CopG family, Saci_0942), a DtxR family protein (Saci_1012), a Tet family protein (Saci_1107), a Lrp/AsnC family protein (Saci_2136), and two HTH domain-containing proteins (Saci_0102 and Saci_0800). Except for the Tet and the Lrp/AsnC family proteins, these transcription factors are conserved in *S. islandicus* REY15A, suggesting that they may play important roles in cell cycle regulation. To test this hypothesis, we focused on

SiRe_0197, an RHH domain protein of *S. islandicus* REY15A. We name it aCcr1 (for Cell cycle regulator 1) based on the results described below.

Ccr1 is a 58-amino acid protein (Fig. S1A) with an isoelectric point of 9.45 and a predicted molecular mass of 6.9 kDa. Similar to other RHH proteins, aCcr1 is predicted to function as a dimer (Schreiter and Drennan, 2007) and interact with the major groove of the dsDNA via two-stranded β-sheet containing positively charged amino acid residues (Fig. S1B). Indeed, we confirmed that the purified aCcr1 protein existed as a dimer in solution using size exclusion chromatography and glutaraldehyde cross-linking (Fig. S2A and S2B).

Transcriptomic analysis of cell cycle-synchronized *S. islandicus* REY15A cells (Liu et al., 2021b) revealed that the transcription levels of aCcr1 and cell division genes *cdvA*, *escrt-III*, and *vps4* exhibits cyclic patterns (Fig. 1). Interestingly, the transcriptional level of *cdvA* peaked at about 60 minutes following the removal of acetic acid, which was used to synchronize the cells in G2 phase, while the levels of aCcr1, *escrt-III* and *vps4* reached their maxima at approximately 120 minutes after the release of the cell cycle arrest. This result is consistent with that based on microarray analysis in *S. acidocaldarius* (Lundgren and Bernander, 2007) and indicates that aCcr1 (SiRe_0197) is likely a cell division specific transcription factor in *Sulfolobus islandicus* REY15A.

To verify the importance of aCcr1 for the cell, we attempted to knock out aCcr1 using an endogenous CRISPR-based genome editing system in *S. islandicus* REY15A (Fig. S3, Li et al., 2016). However, all attempts failed to yield any viable knockout clones, implying that *aCcr1* is probably an essential gene. This result suggests that the putative regulatory role of aCcr1 is indispensable for cell survival.

**Over-expression of aCcr1 results in remarkable cell enlargement and the DNA binding activity of aCcr1 is critical for its cell division regulation**

To probe the *in vivo* function of aCcr1, we attempted to obtain strains with aCcr1 being down- or up-regulated. Unfortunately, there was no suitable protospacer in aCcr1 in *S. islandicus* REY15A for the knockdown analysis according to the endogenous CRISPR-based method (Li et al., 2016; Peng et al., 2017). However, to facilitate the functional analysis of aCcr1, a series of aCcr1 over-expression strains, including those over-expressing the wild type aCcr1 as well as putative DNA-binding deficient mutants aCcr1(R2A), aCcr1(K7A), and aCcr1(R27A) (Fig. S1B), were obtained (Table S1).

Comparing with the control, cells over-expressing aCcr1 showed an obvious growth retardation (Fig. 2A) and exhibited greatly enlarged cell sizes (Fig. 2B and 2C) and increasing amounts of DNA (Fig. 2D). The average diameter of the cells reached a maximum of 4.58 μm at 24 h after induction (Fig. 2C). These phenotypes are indicative of cell division defects in cells over-expressing aCcr1. To verify whether the observed cell division defect is dependent on the DNA binding activity of aCcr1, we compared the growth and cell sizes of the strains over-expressing the wild type aCcr1 and DNA-binding

deficient mutants R2A, K7A, and R27A. As shown in Fig. S4A-4C, all the cells over-expressing the mutant proteins displayed normal growth and cell morphology. The expression of the wild type and mutant aCcr1 proteins was confirmed by Western blotting analysis (Fig. S4D). These results indicated that the positively charged residues play a critical role in the regulation of target gene expression and suggests that the DNA binding activity is essential for cell division regulation.

**The cell division gene *cdvA* is strongly downregulated in cells over-expressing aCcr1**

To identify which genes are transcriptionally regulated by aCcr1 and to gain insight into how aCcr1 over-expression influences the cell division, we conducted comparative transcriptomic analysis of the aCcr1 over-expressing strain and the control carrying an empty vector pSeSD. Samples were taken at 12 h after arabinose induction and subjected to transcriptomic analysis. In total, 76 and 124 genes were up- and downregulated by more than two folds, respectively (Table S3-S4, Fig. 3). If 4-fold was taken as a threshold, 4 and 17 genes were up- and down-regulated, respectively (Fig. 3, Table 1). Intriguingly, *cdvA* (*sire_1173*), the archaea-specific cell division gene (Lindas et al., 2008; Liu et al., 2017; Samson et al., 2008), was among the most highly down-regulated genes (Fig. 3, Table 1). During cell division, CdvA binds to the chromosome and membrane, forming the ring-like structure, then recruits ESCRT-III to the mid-cell for cell division. Over-expression of aCcr1 leads to increase in cell diameter and DNA content, indicative of failure in cell division. A very similar phenotype was obtained when *cdvA* transcription was downregulated using the CRISPR knockdown technology (Liu et al., 2021b). In addition, the gene coding for ePK1 (SiRe_2056) was also among the significantly down-regulated genes (Fig. 3, Table 1).

**Ccr1 binds to the promoters of *cdvA* and other highly down-regulated genes at a conserved motif, aCcr1-box**

To test whether aCcr1 binds to the promoter of *cdvA*, we performed EMSA analysis using $P_{cdvA}$ as a substrate. Purified aCcr1 protein (0, 0.1, 0.2, 0.4, and 0.8 μM) was incubated with fluorescence (FAM)-labelled DNA substrates (Fig. 4A). When an oligonucleotide with the sequence corresponding to the distal region (-100 to -51) of the $P_{cdvA}$ promoter was used as a substrate, no retardation in electrophoretic mobility was observed (Fig. 4A and 4C). In contrast, when the substrate contained the $P_{cdvA}$ sequence proximal to the first *cdvA* codon (-50 to -1), electrophoretic mobility was retarded in a protein concentration dependent manner (Fig. 4A and 4C). Therefore, the aCcr1 binding site was localized to the -50 to -1 region, covering the BRE (TFIIB recognition element), TATA-box, and the TSS (transcription start site) regions. To further characterize the DNA binding activity of aCcr1, we expressed and purified the site-directed mutants of aCcr1, aCcr1(R2A), aCcr1(K7A), and aCcr1(R27A), from *E. coli* (Table S1, Fig. S1B and S5A). All the mutants lost the ability to bind to the *cdvA* promoter (Fig. S5B). Thus, we confirmed that R2, K7, and R27 are critical for promoter binding. In addition, we found that aCcr1 was also able

to bind to $P_{sire_2056}$, a promoter regulating the expression of ePK1-encoding gene *sire_2056* (Fig. S5D).

To understand the substrate binding specificity of aCcr1, we analysed the promoter sequences of all 17 genes repressed in the aCcr1 over-expression strain (Tables 1-2, Fig. 5). Notably, *sire_0018* and *sire_0019* are within the same operon, and so are *sire_0623* and *sire_0624*, whereas a bidirectional promoter sequence is apparently shared by *sire_2056* and *sire_2057* (Fig. 5). All 15 promoter sequences of aCcr1-repressed *S. islandicus* REY15A genes were retrieved and subjected to de novo motif discovery by MEME server. We found that 10 promoters (of 12 genes) contain one or two copies of a 9 bp motif A(T/G)G(A)TA(G)A(T/G)TACN, which we name as aCcr1-box (Fig. 4B and Fig. 5, Table 2).

We confirmed the importance of the motif for aCcr1 binding to the promoters of c*dvA* by EMSA. As shown in Fig. 4C and 4D, deletion of either one aCcr1-box reduced the binding affinity, while deletion or replacement of both motifs greatly impaired the binding of aCcr1. Interestingly, aCcr1-boxes are present in the promoters of *cdvA* homologs from other Sulfolobales species, e.g., *S. acidocaldarius* DSM639 (*saci_1374*), *Acidianus hospitalis* W1 (*ahos_1333*), *Metallosphaera cuprina* Ar-4 (*mcup_0558*), *Sulfuracidifex tepidarius* (*ic006_1093*), and *Stygiolobus azoricus* (*d1868_04805*) (Table 2), suggesting that aCcr1 binding to *cdvA* promoter is conserved in Sulfolobales. To test if the aCcr1 homologs from other crenarchaeal species are functional *in vivo*, we over-expressed in *S. islandicus* REY15A SacCcr1 (Ccr1 from *S. acidocaldarius*), which differs from SisCcr1 by four residues (Y23T, M38L, L43T, and R47T) (Fig. S1A). As expected, the SacCcr1 over-expression strain showed similar phenotype to cells over-expressing SisCcr1 (Fig. S7). Given that aCcr1-box motifs are present in the promoters of *cdvA* genes across Sulfolobales (Table 2), the mechanism of aCcr1-mediated control of cell division through repression of CdvA likely to be conserved as well, at least, in members of the Sulfolobales. We also found that the motif in the promoter of *ePK1* (*sire_2056*) is critical for aCcr1 binding (Fig. S5D). Thus, 13 out of 17 genes with more than 4-fold downregulation could be repressed by aCcr1 binding to the aCcr1-box motif within their promoters. Because most of the sites are located between the TATA-box and the translation start site, binding to the promotor by aCcr1 would prevent the formation of translational pre-initiation complex, leading to transcription repression. While the repression of *cdvA* by aCcr1 is probably the main mechanism for cell division failure in the aCcr1 over-expression strain, the physiological functions of repression of other genes such as *ePK1* by aCcr1 need further investigation.

## Over-expression of aCcr1 affects cell cycle progression due to specific downregulation of *cdvA* and other cell division genes

The growth retardation and cell enlargement phenotypes of the aCcr1 over-expression strain suggested that the cell division genes could be downregulated in the cell. Cell division in Sulfolobales is dependent on the eukaryotic-like ESCRT machinery, which

comprises the archaea-specific protein CdvA, four ESCRT-III homologs (ESCRT-III [CdvB], ESCRT-III-1 [CdvB1], ESCRT-III-2 [CdvB2], ESCRT-III-3 [CdvB3]), and an AAA+ ATPase Vps4 (also known as CdvC) (Lindas et al., 2008; Liu et al., 2017; Samson et al., 2008). CdvA binds to DNA and membrane (Moriscot et al., 2011; Samson et al., 2011) and then recruits ESCRT-III to the mid-cell, which forms a ring-like structure and drives cell division (Samson et al., 2011). Vps4 binds to ESCRT-III and other ESCRT-III homologs (Liu et al., 2017) and, upon ATP hydrolysis, drives the disassembly of the contractile ESCRT-III ring, thereby promoting the cell division process (Samson et al., 2008; Tarrason Risa et al., 2020). In a previous study, we reported that infection of *S. islandicus* REY15A with STSV2 led to transcriptional downregulation of cell division genes, including *cdvA*, *escrt-III, escrt-III-1, escrt-III-2, escrt-III-3* and vps4, which resulted in dramatic increase in the size and DNA content of infected cells (Liu et al., 2021a). To confirm the role of aCcr1 in cell division regulation and to investigate the effect of aCcr1 over-expression on cell division proteins, we examined the relative transcriptional levels of the corresponding genes by RT-qPCR. As shown in Fig. 6A, all of the above mentioned cell division genes were significantly repressed. Among them, *cdvA* was affected most strongly. To detect if aCcr1 over-expression also affects the expression of genes in the upstream cell cycle process, we examined the expression levels of chromosome segregation genes *segA* and *segB* (Yen et al., 2021), but no significant changes were found (Fig. 6B), suggesting that over-expression of aCcr1 does not affect the process of chromosome segregation.

To further confirm the regulatory role of aCcr1 in cell cycle progression, we analysed the aCcr1 over-expression strain by flow cytometry using synchronized cells. We added D-arabinose 3 h after the addition of acetic acid (Fig. 7A). The expression of aCcr1 was induced 1.0 h before the acetic acid was removed, as confirmed by Western blotting. *S. islandicus* REY15A (E233S) containing the empty plasmid was used as a control. As shown in (Fig. 7B), subpopulation of cells containing a single chromosome copy (1C) could be observed at 0-4 h and up to the end of the normal cell cycle in the control, but not in the aCcr1 over-expression strain. Thus, over-expression of aCcr1 inhibited cell division. Western blotting results showed that in the control cells, CdvA exhibited a cyclic pattern with higher expression at 0-1 h (Fig. 7C). In contrast, the CdvA levels remained low in the aCcr1 over-expression cells, consistent with the RT-qPCR results. Thus, we established that binding of aCcr1 to the promoter of *cdvA* represses the gene expression and reduces CdvA level in the cell, leading to cell division failure.

### Ccr1 over-expression jeopardizes contractile ring formation

To further characterize how the cell division is affected by the over-expression of aCcr1, we performed fluorescence microscopy analysis on the synchronized cells over-expressing aCcr1 using anti-ESCRT-III antibodies. Cells cultured at 3-4 h after removal of acetic acid were sampled and analysed. In the control cells carrying the empty vector, ESCRT-III displayed mid-cell localization and formed ring-like structures in 7.2% of the cells (Fig. 7D). In the aCcr1 over-expressing strain, ESCRT-III ring was barely visible (0.8%), probably because in the absence of CdvA, ESCRT-III cannot be recruited to the

membrane (Fig. 7D). This result further reinforces the hypothesis that aCcr1 regulates cell division via *cdvA* repression.

## Ccr1 homologs are widespread in Sulfolobales and their viruses

To explore the diversity and distribution of aCcr1 in the domain of Archaea, we performed PSI-BLAST search using aCcr1 from *S. islandicus* REY15A as a query. Given that RHH domain proteins are widespread in archaea and orthology of short divergent proteins is not straightforward to assess, we restricted our focus to proteins displaying relatively high sequence similarity to aCcr1 and which could be retrieved after two iterations of PSI-BLAST. The search yielded multiple hits in hyperthermophilic crenarchaea of the orders Sulfolobales and Desulfurococcales (Fig. 8). We note, however, that further search iterations revealed additional homologs in a broader diversity of archaea, including those from other phyla. In Sulfolobales genomes, aCcr1 genes are encoded within orthologous loci and have conserved gene synteny (Fig. S6). Interestingly, all *cdvA* promoter sequences of the Sulfolobales species contain at least one aCcr1-box motif at a conserved position (Table 2).

Intriguingly, aCcr1 homologs are also conserved in several conjugative plasmids and genomes of Sulfolobales viruses from five different families, including *Rudiviridae*, *Bicaudaviridae*, *Fuselloviridae*, *Ungulaviridae* and *Turriviridae* (Prangishvili et al., 2017) as well as in unclassified Sulfolobales viruses YNP1 and YNP2 (Fig. 8). The viral, plasmid and cellular aCcr1 homologs display a complex evolutionary history with multiple horizontal gene transfers, even within the same family of viruses. The phylogeny splits into three major clades (I-III), with members of the Sulfolobales being distributed between clades I and III, and Desulfurococcales forming the clade II (Fig. 8). Viruses are intermixed with the Sulfolobales within clades I and III, whereas plasmids are restricted to clade III. The horizontal gene transfer of aCcr1 homologs between viruses and cells suggests that viruses might have hijacked aCcr1 genes for manipulation of the cell cycle of their hosts.

## Over-expression of viral aCcr1 homologs impairs cell cycle progression in *S. islandicus* REY15A

To investigate the functions of viral aCcr1 homologs, we have chosen four viruses belonging to clade I, which also includes aCcr1 of *S. islandicus* REY15A and *S. acidocaldarius* (Fig. 8). In particular, we constructed strains over-expressing aCcr1 homologs from *Acidianus* two-tailed virus (ATV_gp29), *Sulfolobus* monocaudavirus 3 (SMV3_gp63), *Sulfolobus islandicus* rod-shaped virus 2 (SIRV2_gp21), and *Sulfolobus* turreted icosahedral virus 2 (STIV2_B60). The former two viruses belong to the same family as STSV2, which has been recently demonstrated to induce cell enlargement upon infection (Liu et al., 2021a), while the latter two are lytic viruses that do not induce obvious cell size alterations (Happonen et al., 2010; Kessler et al., 2004) Over-expression of the ATV_gp29 and SMV3_gp63 resulted in growth retardation and yielded enlarged cells with multiple chromosomes (Fig. 9, S8C), reminiscent of the cell phenotype induced by STSV2

and SMV1 infections (Liu et al., 2021a). By contrast, the growth of transformants carrying plasmids pSeSD-SIRV2_gp21 and pSeSD-STIV2_B60 homologs, respectively, did not have apparent effect on the cell growth and morphology (Fig. S8A and S8B). We checked the protein expression of the trains carrying each of four plasmid by Western blotting. The result showed that the proteins were expressed except SIRV2_gp21 (Fig. S8C). We then checked the DNA binding activity to P*cdvA*, purified ATV_gp29, SMV3_gp63, and SIRV2_gp21 proteins (expressed from *E. coli)* can bind to the $P_{cdvA}$ promoter, whereas and STIV2_B60 cannot (Fig. S5C). Careful examination of the amino sequence of STIV2, we found one of the putative DNA binding site arginine 2 is replaced with glutamine (Fig. S1A), which may explain why STIV2_B60 had no binding to P*cdvA.* Thus, these results suggest a mechanism by which viruses, particularly, bicaudaviruses, can control the division of their host cells. By using a small RHH family cell division regulator, probably obtained by horizontal gene transfer from their hosts, the viruses can manipulate the cell cycle, transforming the cell into a giant virion producing factory for viral production.

## Discussion

Studies on the cell cycle progression and regulation in archaea could provide a key to understanding the eukaryogenesis, one of the most intriguing mysteries in biology. Recent research has shown that archaea of the Asgard superphylum, in particular, Heimdallarchaeota, are evolutionarily most closely related to eukaryotes (Imachi et al., 2020; Liu et al., 2021c; Zaremba-Niedzwiedzka et al., 2017). However, microorganisms from the Asgard superphylum are difficult to cultivate and no genetically tractable system has been established, which hinders the characterization of the putative archaeal ancestor of eukaryotes. Archaea of the TACK superphylum share many features with the Asgard superphylum and could serve as valuable models for understanding the evolution of eukaryotic-like features in archaea. In particular, genetically tractable members of the genera *Sulfolobus* and *Saccharolobus* represent one of such archaeal model systems with many eukaryotic signature proteins and a eukaryotic-like cell cycle (Bernander and Poplawski, 1997; Spang et al., 2017). Mapping of cell cycle regulatory mechanisms and identification of proteins involved in cell-cycle processes in these model archaea is crucial for understanding the basic biology of archaea (Lundgren and Bernander, 2007) and the origin of Eukaryota. In this study, we identified a small RHH family transcription factor, named aCcr1, from *Sulfolobales* and their viruses that can control the cell division of *Saccharolobus islandicus*. It binds to a conserved 9-bp palindromic motif, aCcr1-box, within the promoter of *cdvA*, an archaea-specific component of the cell division machinery, thereby repressing the *cdvA* expression. Notably, sequence analysis showed that the aCcr1-box is present in all Sulfolobales *cdvA* promoters at equivalent positions. Thus, we hypothesize that aCcr1-mediated cell cycle control through repression of CdvA is conserved in this archaeal order.

In euryarchaea, the FtsZ-based bacterial-like system is utilized for the cell division (Caspi and Dekker, 2018; Lindas et al., 2008; Samson et al., 2011). In halophilic euryarchaea, an RHH family transcription factor, CdrS, plays a central role in the regulation of the cell

division. Similar to aCcr1 of *S. islandicus*, *cdrS* is essential in *Haloferax volcanii* and could not be deleted. It is a global transcriptional regulator, controlling expression of *ftsZ*. It also regulates the expression of genes linked to other metabolic and regulatory processes, likely allowing cells to properly coordinate growth, division, and metabolic activity (Liao et al., 2021a, 2021b). CdrS binds upstream of the promoters of *ftsZ1* and *dacZ* (encoding a diadenylate cyclase, DacZ), which synthesizes the second messenger molecule c-di-AMP, and three genes related to proteasome function (*cdc48d*, *panA*, and *psmB*) (Liao et al., 2021a; Liao et al., 2021b). In another halophile, *Halobacterium salinarum*, the gene coding for the CdrS is co-transcribed with the cell division gene *ftsZ2,* and the gene encoding CdrL, another RHH transcription factor which binds the promoter of *cdrS-ftsZ* (Darnell et al., 2020). Interestingly, in this haloarchaeon, the *cdrS* can be deleted and appears not to be involved in the regulation of DacZ and proteasome proteins, which might explain its dispensability (Darnell et al., 2020). The *cdrS-ftsZ2* locus is well conserved across the Euryarchaeota, especially within the Halobacteria (Darnell et al., 2020) (Fig. S9), suggesting a general cell division regulation mechanism in euryarchaea.

There are many obvious parallels between aCcr1 and CdrS. In particular, both aCcr1 and CdrS are small RHH transcription factors and although they are distantly related at the amino acid sequence level, the modelled three-dimensional structures are very similar (Fig. S1C). Furthermore, the aCcr1-box is similar to the most conserved part of the putative CdrS binding motif (also a palindromic sequence) (Liao et al., 2021b). Finally, CdrS and aCcr1 play equivalent roles in the control of cell cycle progression. We hypothesize that the aCcr1/CdrS-mediated cell division regulation mechanism has evolved before the divergence of archaeal lineages using the ESCRT-III-based and FtsZ-based cell division systems.

Apart from *cdvA*, 11 other genes were repressed by aCcr1. We have confirmed that the conserved aCcr1-box motif was responsible for aCcr1 binding to the *ePK1* promoter. The ePK1 from *S. islandicus* and its homolog in *S. acidocaldarius* exhibited DNA damage agent-dependent changes at transcriptional level or in phosphorylation status (Gotz et al., 2007; Huang et al., 2020; Sun et al., 2018). Phosphorylation plays a crucial role in the cell cycle regulation in eukaryotic cells, and could play a similar role in archaea. For instance, repression of *ePK1* could regulate the cell cycle through protein phosphorylation. Functions for the other 10 proteins for which the promoters contain aCcr1-box include possible nutrient uptake related proteins (endoglucanase, SiRe_0332, and thermopsin-like protease, SiRe_0691) and a predicted component of anti-virus defence system ATPase (SiRe_0086) (Table 1). Further characterization of the regulation of these genes by aCcr1 could help unravel the cell cycle regulation network in Archaea.

Many aCcr1 homologs are present in the genomes of archaeal viruses (Fig. 8). Over-expression of the aCcr1 homologs from the *Acidianus* two-tailed virus (ATV_gp29) and *Sulfolobus* monocaudavirus 3 (SMV3_gp63) resulted in growth retardation and appearance of enlarged cells with multiple chromosomes (Fig. 9). *Acidianus* two-tailed virus and *Sulfolobus* monocaudavirus 3 are spindle-shaped viruses which also include

genetically distant but morphologically similar *S. tengchongensis* spindle-shaped virus 1 (STSV1), *S. tengchongensis* spindle-shaped virus 2 (STSV2), *Acidianus* tailed spindle virus (ATSV), and *Sulfolobus* monocaudavirus 1 (SMV1), all members of the family *Bicaudaviridae* (Prangishvili et al., 2018). We previously reported a virus-induced cell enlargement of *S. islandicus* REY15A by SMV1 and STSV2, illuminating the inherent plasticity of *Sulfolobus* cells, which might be relevant for eukaryogenesis (Liu et al., 2021a). Although the regulators manipulating cell division in STSV2 and SMV1 are yet to be identified, the finding that ATV- and SMV3-encoded aCcr1 homologs induce cell enlargement suggests that a similar mechanism might be operating in STSV2- and SMV1-infected cells. By hijacking a key cell division regulator, viruses can manipulate archaeal cell cycle, transforming the cell into a giant virion producing factory. A similar scenario might have also taken place in ancestral archaea, producing cells with sufficiently large volume, a prerequisite for eukaryogenesis.

Global transcriptional analysis revealed that transcription of aCcr1 and cell division proteins CdvA, ESCRT-III and Vps4 are cyclically controlled in *S. acidocaldarius* (Lundgren and Bernander, 2007). Interestingly, the peak of aCcr1 (Saci_0942) transcription was about 30 minutes after that for CdvA, but coincided with those of ESCRT-III and Vps4. In our transcriptomic analysis, a similar pattern was also observed (Fig. 1B). Based on these results, we propose a scenario of cell division control by aCcr1 in *S. islandicus* REY15A. After cell division is initiated by CdvA, aCcr1 expression is activated by an unidentified factor, leading to a timely shut down of the CdvA expression (Liu et al., 2021b). This will prevent further recruitment of ESCRT-III to the membrane at the mid-cell and ensure that the cell division ring assembles only during the cytokinesis stage of the cell cycle. In summary, we have identified a key cell division regulator, a small RHH family protein aCcr1 that controls cell division in crenarchaea through repression of the early cell division protein in the cytokinesis machinery. This study open doors for further dissection of the cell cycle regulation network in archaea.

## Acknowledgements

This work was supported by the National Key Research and Development Program of China (No. 2020YFA0906800), the National Natural Science Foundation of China (No. 31970546 and 31670061 to YS, 31970119 to JN, and 31771380 to QS) and the State Key Laboratory of Microbial Technology. Work in the MK laboratory was supported by a grant from Ville de Paris (Emergence(s) project MEMREMA). We would like to thank all the lab members of the CRISPR and Archaea Biology Research Centre for helpful discussions.

## References

1. Altschul, S.F., Madden, T.L., Schaffer, A.A., Zhang, J., Zhang, Z., Miller, W., and Lipman, D.J. (1997). Gapped BLAST and PSI-BLAST: a new generation of protein database search programs. Nucleic Acids Res *25*, 3389-3402.
2. Bernander, R. (2000). Chromosome replication, nucleoid segregation and cell division

in archaea. Trends Microbiol *8*, 278-283.
3. Bernander, R., and Poplawski, A. (1997). Cell cycle characteristics of thermophilic archaea. J Bacteriol *179*, 4963-4969.
4. Capella-Gutierrez, S., Silla-Martinez, J.M., and Gabaldon, T. (2009). trimAl: a tool for automated alignment trimming in large-scale phylogenetic analyses. Bioinformatics *25*, 1972-1973.
5. Caspi, Y., and Dekker, C. (2018). Dividing the Archaeal Way: The Ancient Cdv Cell-Division Machinery. Front Microbiol *9*, 174.
6. Chu, Y., Zhu, Y., Chen, Y., Li, W., Zhang, Z., Liu, D., Wang, T., Ma, J., Deng, H., Liu, Z.J.*, et al.* (2016). aKMT Catalyzes Extensive Protein Lysine Methylation in the Hyperthermophilic Archaeon Sulfolobus islandicus but is Dispensable for the Growth of the Organism. Mol Cell Proteomics *15*, 2908-2923.
7. Darnell, C.L., Zheng, J., Wilson, S., Bertoli, R.M., Bisson-Filho, A.W., Garner, E.C., and Schmid, A.K. (2020). The Ribbon-Helix-Helix Domain Protein CdrS Regulates the Tubulin Homolog ftsZ2 To Control Cell Division in Archaea. mBio *11*.
8. Deng, L., Zhu, H., Chen, Z., Liang, Y.X., and She, Q. (2009). Unmarked gene deletion and host-vector system for the hyperthermophilic crenarchaeon Sulfolobus islandicus. Extremophiles *13*, 735-746.
9. Dewachter, L., Verstraeten, N., Fauvart, M., and Michiels, J. (2018). An integrative view of cell cycle control in Escherichia coli. FEMS Microbiol Rev *42*, 116-136.
10. Dexl, S., Reichelt, R., Kraatz, K., Schulz, S., Grohmann, D., Bartlett, M., and Thomm, M. (2018). Displacement of the transcription factor B reader domain during transcription initiation. Nucleic Acids Res *46*, 10066-10081.
11. Diaz-Moralli, S., Tarrado-Castellarnau, M., Miranda, A., and Cascante, M. (2013). Targeting cell cycle regulation in cancer therapy. Pharmacol Ther *138*, 255-271.
12. Evans, T., Rosenthal, E.T., Youngblom, J., Distel, D., and Hunt, T. (1983). Cyclin: a protein specified by maternal mRNA in sea urchin eggs that is destroyed at each cleavage division. Cell *33*, 389-396.
13. Gabler, F., Nam, S.Z., Till, S., Mirdita, M., Steinegger, M., Soding, J., Lupas, A.N., and Alva, V. (2020). Protein Sequence Analysis Using the MPI Bioinformatics Toolkit. Curr Protoc Bioinformatics *72*, e108.
14. Galderisi, U., Jori, F.P., and Giordano, A. (2003). Cell cycle regulation and neural differentiation. Oncogene *22*, 5208-5219.
15. Gotz, D., Paytubi, S., Munro, S., Lundgren, M., Bernander, R., and White, M.F. (2007). Responses of hyperthermophilic crenarchaea to UV irradiation. Genome Biol *8*, R220.
16. Guindon, S., Dufayard, J.F., Lefort, V., Anisimova, M., Hordijk, W., and Gascuel, O. (2010). New algorithms and methods to estimate maximum-likelihood phylogenies: assessing the performance of PhyML 3.0. Syst Biol *59*, 307-321.
17. Guo, L., Brugger, K., Liu, C., Shah, S.A., Zheng, H., Zhu, Y., Wang, S., Lillestol, R.K., Chen, L., Frank, J.*, et al.* (2011). Genome analyses of Icelandic strains of Sulfolobus islandicus, model organisms for genetic and virus-host interaction studies. J Bacteriol *193*, 1672-1680.
18. Happonen, L.J., Redder, P., Peng, X., Reigstad, L.J., Prangishvili, D., and Butcher, S.J. (2010). Familial relationships in hyperthermo- and acidophilic archaeal viruses. J Virol

*84*, 4747-4754.
19. Hoffmann, L., Anders, K., Bischof, L.F., Ye, X., Reimann, J., Khadouma, S., Pham, T.K., van der Does, C., Wright, P.C., Essen, L.O.*, et al.* (2019). Structure and interactions of the archaeal motility repression module ArnA-ArnB that modulates archaellum gene expression in Sulfolobus acidocaldarius. J Biol Chem *294*, 7460-7471.
20. Huang, Q., Lin, Z., Wu, P., Ni, J., and Shen, Y. (2020). Phosphoproteomic Analysis Reveals Rio1-Related Protein Phosphorylation Changes in Response to UV Irradiation in Sulfolobus islandicus REY15A. Front Microbiol *11*, 586025.
21. Huang, Q., Mayaka, J.B., Zhong, Q., Zhang, C., Hou, G., Ni, J., and Shen, Y. (2019). Phosphorylation of the Archaeal Holliday Junction Resolvase Hjc Inhibits Its Catalytic Activity and Facilitates DNA Repair in Sulfolobus islandicus REY15A. Front Microbiol *10*, 1214.
22. Huang, Q., Zhong, Q., Mayaka, J.B.A., Ni, J., and Shen, Y. (2017). Autophosphorylation and Cross-Phosphorylation of Protein Kinases from the Crenarchaeon Sulfolobus islandicus. Front Microbiol *8*, 2173.
23. Imachi, H., Nobu, M.K., Nakahara, N., Morono, Y., Ogawara, M., Takaki, Y., Takano, Y., Uematsu, K., Ikuta, T., Ito, M.*, et al.* (2020). Isolation of an archaeon at the prokaryote-eukaryote interface. Nature *577*, 519-525.
24. Katoh, K., Rozewicki, J., and Yamada, K.D. (2019). MAFFT online service: multiple sequence alignment, interactive sequence choice and visualization. Brief Bioinform *20*, 1160-1166.
25. Kessler, A., Brinkman, A.B., van der Oost, J., and Prangishvili, D. (2004). Transcription of the rod-shaped viruses SIRV1 and SIRV2 of the hyperthermophilic archaeon sulfolobus. J Bacteriol *186*, 7745-7753.
26. Lemmens, L., Maklad, H.R., Bervoets, I., and Peeters, E. (2019). Transcription Regulators in Archaea: Homologies and Differences with Bacterial Regulators. J Mol Biol *431*, 4132-4146.
27. Lewis, M., and Stracker, T.H. (2021). Transcriptional regulation of multiciliated cell differentiation. Semin Cell Dev Biol *110*, 51-60.
28. Li, Y., Pan, S., Zhang, Y., Ren, M., Feng, M., Peng, N., Chen, L., Liang, Y.X., and She, Q. (2016). Harnessing Type I and Type III CRISPR-Cas systems for genome editing. Nucleic Acids Res *44*, e34.
29. Liao, Y., Ithurbide, S., Evenhuis, C., Lowe, J., and Duggin, I.G. (2021a). Cell division in the archaeon Haloferax volcanii relies on two FtsZ proteins with distinct functions in division ring assembly and constriction. Nat Microbiol *6*, 594-605.
30. Liao, Y., Vogel, V., Hauber, S., Bartel, J., Alkhnbashi, O.S., Maass, S., Schwarz, T.S., Backofen, R., Becher, D., Duggin, I.G.*, et al.* (2021b). CdrS Is a Global Transcriptional Regulator Influencing Cell Division in Haloferax volcanii. mBio *12*, e0141621.
31. Lindas, A.C., and Bernander, R. (2013). The cell cycle of archaea. Nat Rev Microbiol *11*, 627-638.
32. Lindas, A.C., Karlsson, E.A., Lindgren, M.T., Ettema, T.J., and Bernander, R. (2008). A unique cell division machinery in the Archaea. Proc Natl Acad Sci U S A *105*, 18942-18946.
33. Liu, J., Cvirkaite-Krupovic, V., Baquero, D.P., Yang, Y., Zhang, Q., Shen, Y., and

Krupovic, M. (2021a). Virus-induced cell gigantism and asymmetric cell division in archaea. Proc Natl Acad Sci U S A *118*.
34. Liu, J., Cvirkaite-Krupovic, V., Commere, P.H., Yang, Y., Zhou, F., Forterre, P., Shen, Y., and Krupovic, M. (2021b). Archaeal extracellular vesicles are produced in an ESCRT-dependent manner and promote gene transfer and nutrient cycling in extreme environments. ISME J *15*, 2892-2905.
35. Liu, J., Gao, R., Li, C., Ni, J., Yang, Z., Zhang, Q., Chen, H., and Shen, Y. (2017). Functional assignment of multiple ESCRT-III homologs in cell division and budding in Sulfolobus islandicus. Mol Microbiol *105*, 540-553.
36. Liu, Y., Makarova, K.S., Huang, W.C., Wolf, Y.I., Nikolskaya, A.N., Zhang, X., Cai, M., Zhang, C.J., Xu, W., Luo, Z*., et al.* (2021c). Expanded diversity of Asgard archaea and their relationships with eukaryotes. Nature *593*, 553-557.
37. Lundgren, M., and Bernander, R. (2007). Genome-wide transcription map of an archaeal cell cycle. Proc Natl Acad Sci U S A *104*, 2939-2944.
38. Minh, B.Q., Schmidt, H.A., Chernomor, O., Schrempf, D., Woodhams, M.D., von Haeseler, A., and Lanfear, R. (2020). IQ-TREE 2: New Models and Efficient Methods for Phylogenetic Inference in the Genomic Era. Mol Biol Evol *37*, 1530-1534.
39. Morgan, D.O. (1995). Principles of CDK regulation. Nature *374*, 131-134.
40. Moriscot, C., Gribaldo, S., Jault, J.M., Krupovic, M., Arnaud, J., Jamin, M., Schoehn, G., Forterre, P., Weissenhorn, W., and Renesto, P. (2011). Crenarchaeal CdvA forms double-helical filaments containing DNA and interacts with ESCRT-III-like CdvB. PLoS One *6*, e21921.
41. Peng, N., Han, W., Li, Y., Liang, Y., and She, Q. (2017). Genetic technologies for extremely thermophilic microorganisms of Sulfolobus, the only genetically tractable genus of crenarchaea. Sci China Life Sci *60*, 370-385.
42. Prangishvili, D., Bamford, D.H., Forterre, P., Iranzo, J., Koonin, E.V., and Krupovic, M. (2017). The enigmatic archaeal virosphere. Nat Rev Microbiol *15*, 724-739.
43. Prangishvili, D., Krupovic, M., and Ictv Report, C. (2018). ICTV Virus Taxonomy Profile: Bicaudaviridae. J Gen Virol *99*, 864-865.
44. Reimann, J., Lassak, K., Khadouma, S., Ettema, T.J., Yang, N., Driessen, A.J., Klingl, A., and Albers, S.V. (2012). Regulation of archaella expression by the FHA and von Willebrand domain-containing proteins ArnA and ArnB in Sulfolobus acidocaldarius. Mol Microbiol *86*, 24-36.
45. Samson, R.Y., Obita, T., Freund, S.M., Williams, R.L., and Bell, S.D. (2008). A role for the ESCRT system in cell division in archaea. Science *322*, 1710-1713.
46. Samson, R.Y., Obita, T., Hodgson, B., Shaw, M.K., Chong, P.L., Williams, R.L., and Bell, S.D. (2011). Molecular and structural basis of ESCRT-III recruitment to membranes during archaeal cell division. Mol Cell *41*, 186-196.
47. Schreiter, E.R., and Drennan, C.L. (2007). Ribbon-helix-helix transcription factors: variations on a theme. Nat Rev Microbiol *5*, 710-720.
48. Spang, A., Caceres, E.F., and Ettema, T.J.G. (2017). Genomic exploration of the diversity, ecology, and evolution of the archaeal domain of life. Science *357*.
49. Sun, M., Feng, X., Liu, Z., Han, W., Liang, Y.X., and She, Q. (2018). An Orc1/Cdc6 ortholog functions as a key regulator in the DNA damage response in Archaea.

Nucleic Acids Res *46*, 6697-6711.
50. Tarrason Risa, G., Hurtig, F., Bray, S., Hafner, A.E., Harker-Kirschneck, L., Faull, P., Davis, C., Papatziamou, D., Mutavchiev, D.R., Fan, C.*, et al.* (2020). The proteasome controls ESCRT-III-mediated cell division in an archaeon. Science *369*.
51. Vorontsov, E.A., Rensen, E., Prangishvili, D., Krupovic, M., and Chamot-Rooke, J. (2016). Abundant Lysine Methylation and N-Terminal Acetylation in Sulfolobus islandicus Revealed by Bottom-Up and Top-Down Proteomics. Mol Cell Proteomics *15*, 3388-3404.
52. Westfall, C.S., and Levin, P.A. (2017). Bacterial Cell Size: Multifactorial and Multifaceted. Annu Rev Microbiol *71*, 499-517.
53. Willis, L., and Huang, K.C. (2017). Sizing up the bacterial cell cycle. Nat Rev Microbiol *15*, 606-620.Yen, C.Y., Lin, M.G., Chen, B.W., Ng, I.W., Read, N., Kabli, A.F., Wu, C.T., Shen, Y.Y., Chen, C.H., Barilla, D.*, et al.* (2021). Chromosome segregation in Archaea: SegA- and SegB-DNA complex structures provide insights into segrosome assembly. Nucleic Acids Res *49*, 13150-13164.
54. Yue, L., Li, J., Zhang, B., Qi, L., Li, Z., Zhao, F., Li, L., Zheng, X., and Dong, X. (2020). The conserved ribonuclease aCPSF1 triggers genome-wide transcription termination of Archaea via a 3'-end cleavage mode. Nucleic Acids Res *48*, 9589-9605.
55. Zaremba-Niedzwiedzka, K., Caceres, E.F., Saw, J.H., Backstrom, D., Juzokaite, L., Vancaester, E., Seitz, K.W., Anantharaman, K., Starnawski, P., Kjeldsen, K.U.*, et al.* (2017). Asgard archaea illuminate the origin of eukaryotic cellular complexity. Nature *541*, 353-358.

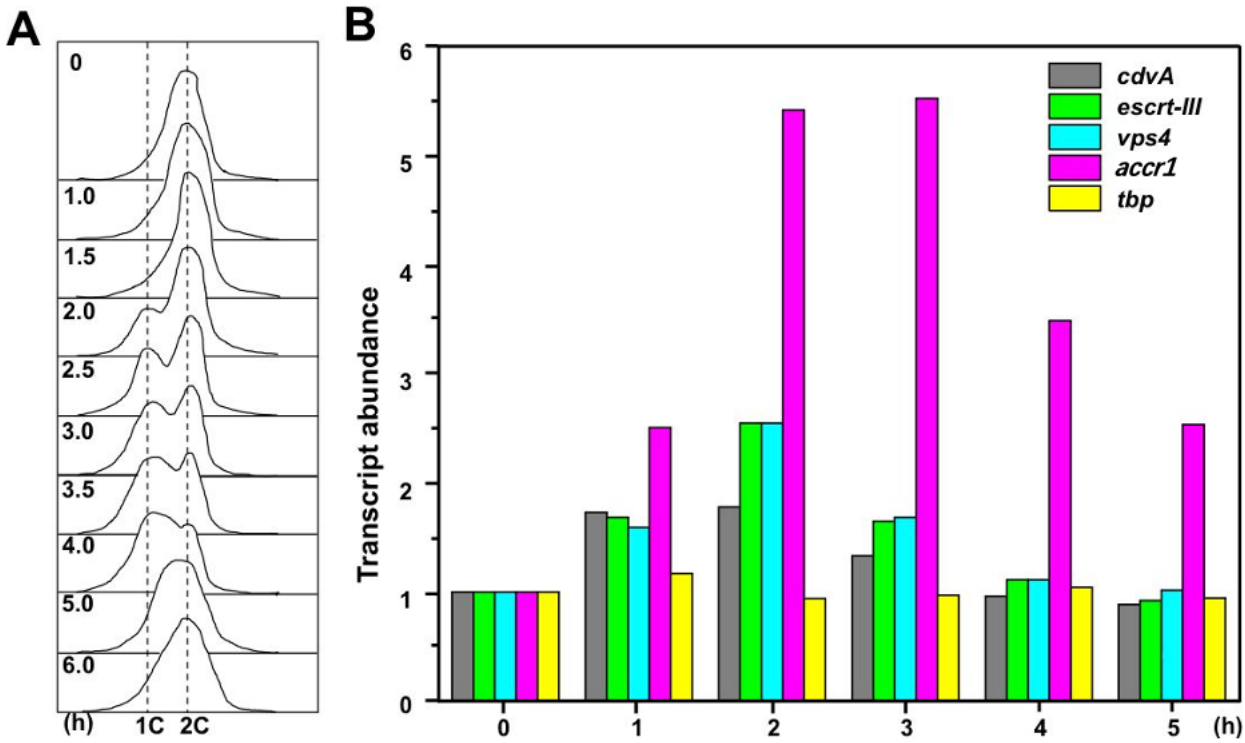


**Figure 1. The gene *accr1* is cyclically transcribed.** (**A**) Flow cytometry profiles of samples of a synchronized *S. islandicus* REY15A (E233S) culture in one cell cycle. The cells were synchronized at G2 phase after treated with 6 mM acetic acid for 6 h before released by removing the acetic acid. The cultures were collected at different time points (0, 1.0, 1.5, 2.0, 2.5, 3.0, 3.5, 4.0, 5.0, and 6.0 h) and subjected to flow cytometry analysis. Cells started to divide at 2.0 h as the appearance of cells with one copy of chromosome (1C) and the ratio of dividing cells reached the highest at about 3-3.5 h. As cell cycle proceeded, cells with two copies of chromosomes (2C) became dominant at 5 h. (**B**) Changes of transcription levels of *accr1* and the cell division genes based on the transcriptomic data of the synchronized cell culture. The cells were collected at 0, 1, 2, 3, 4, and 5 h after cell arrest release.

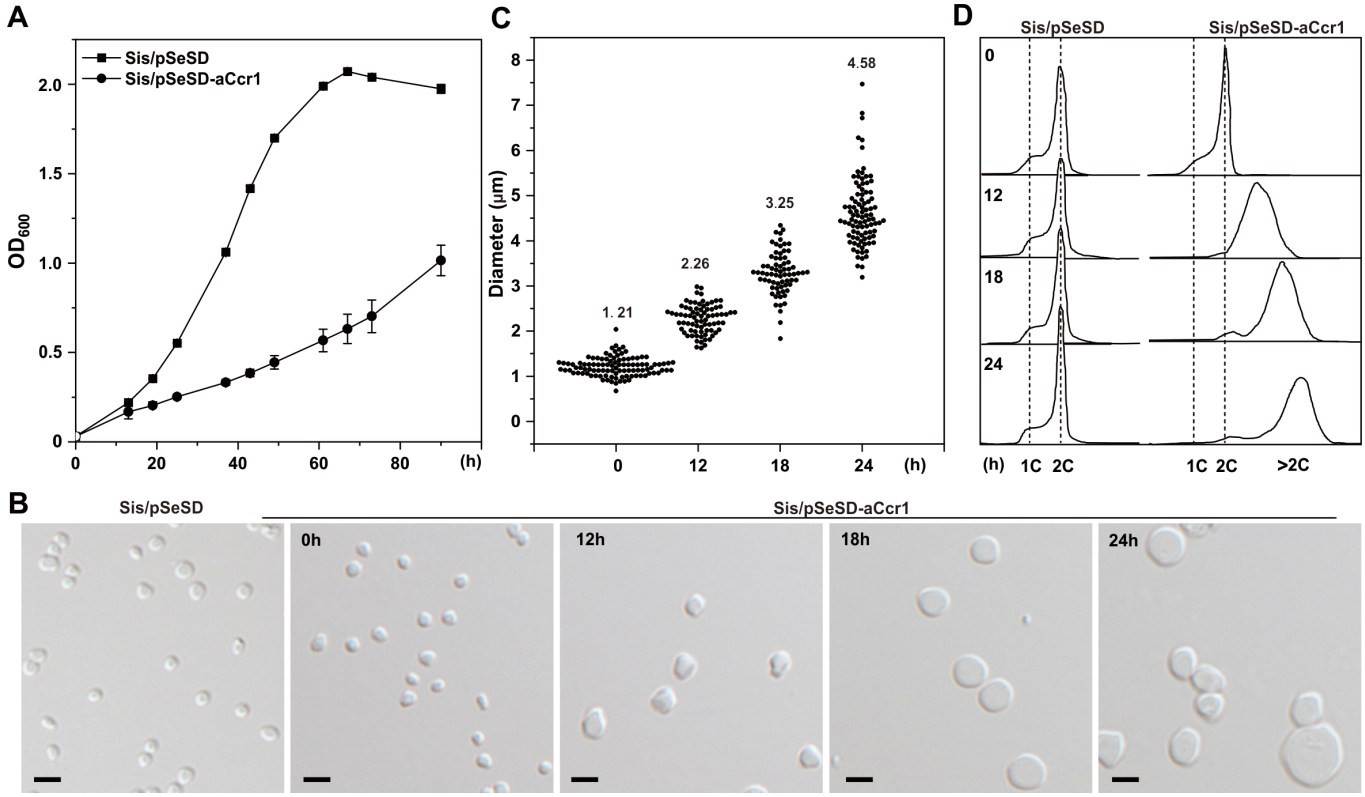


**Figure 2. Overexpression of aCcr1 leads to remarkable cell enlargement.** (A) Growth curves of cells over-expressing C-terminal His-tagged aCcr1. The cells were inoculated into 30 ml induction medium ATV to a final estimated $OD_{600}$ of 0.03. The growth was monitored using spectrometer. Each value was based on data from three independent measurements. Cell harboring the empty plasmid pSeSD was used as a control. (B) Phase contrast microscopy of cells over-expressing aCcr1. Cells cultured in the induction medium were taken at different time points and observed under a NIKON-E microscope. Scale bars: 2 μm. (C) Cell size statistics of the data in (B). Cell cultures were sampled at the indicated time points and observed under the microscope. The diameters of ~100 cells were measured using ImageJ software for each culture repeat. (D) Flow cytometry analysis of the DNA content of Sis/pSeSD and Sis/pSeSD-aCcr1 cells cultured in MATV media.

Sis/pSeSD VS Sis/pSeSD-aCcr1

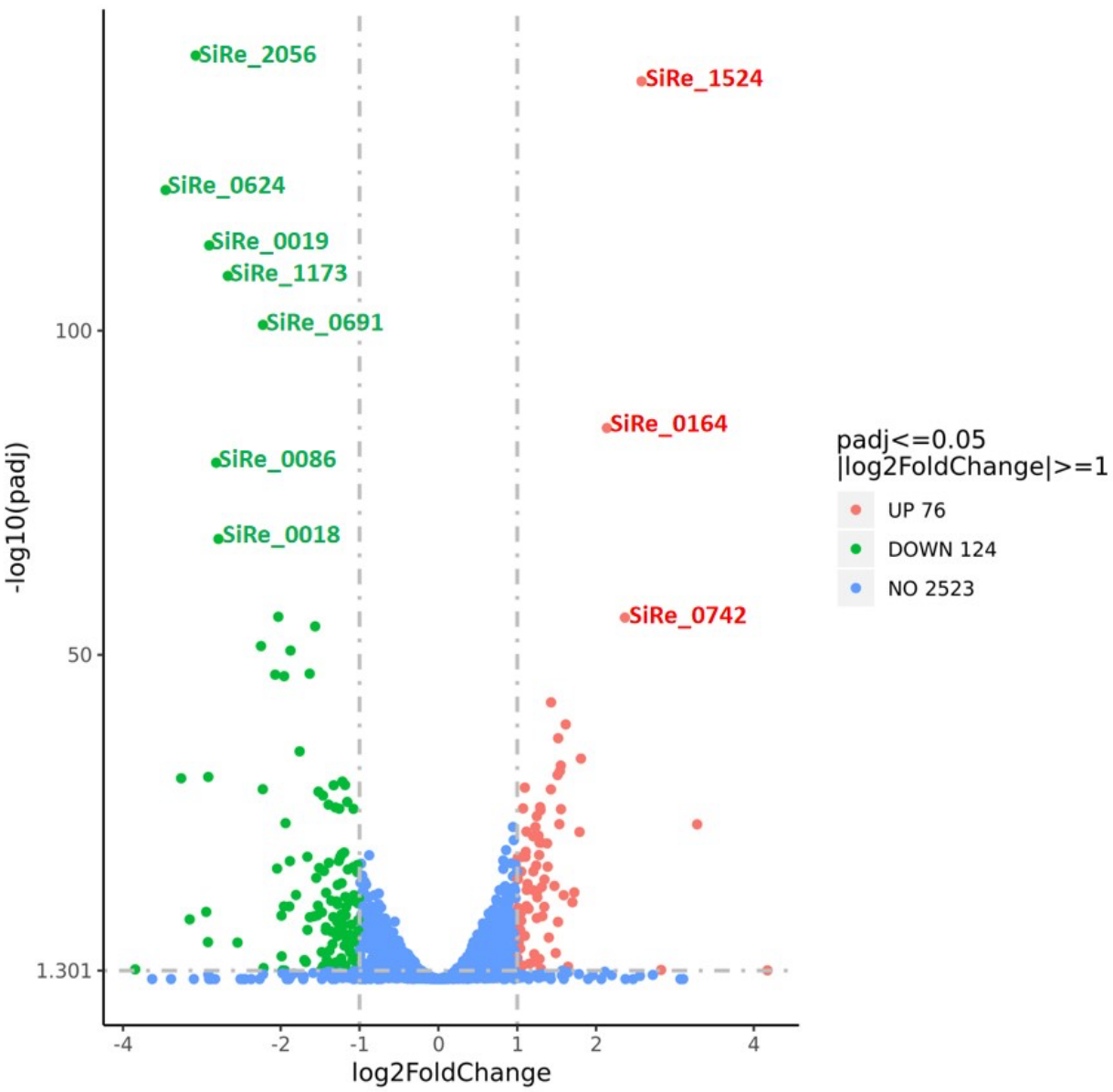


**Figure 3. Volcano plot of differentially expressed genes in strain Sis/pSeSD-aCcr1 compared to the control Sis/pSeSD.** X-axis, fold change in gene expression. Y-axis, significance of fold change. Genes exhibiting >2-fold (i.e. –1 > log2 > +1) up-and down-regulated with significance are highlighted in red and green, respectively, whereas those that showed a <2-fold change in differential gene expression or with no significance are shown in blue.

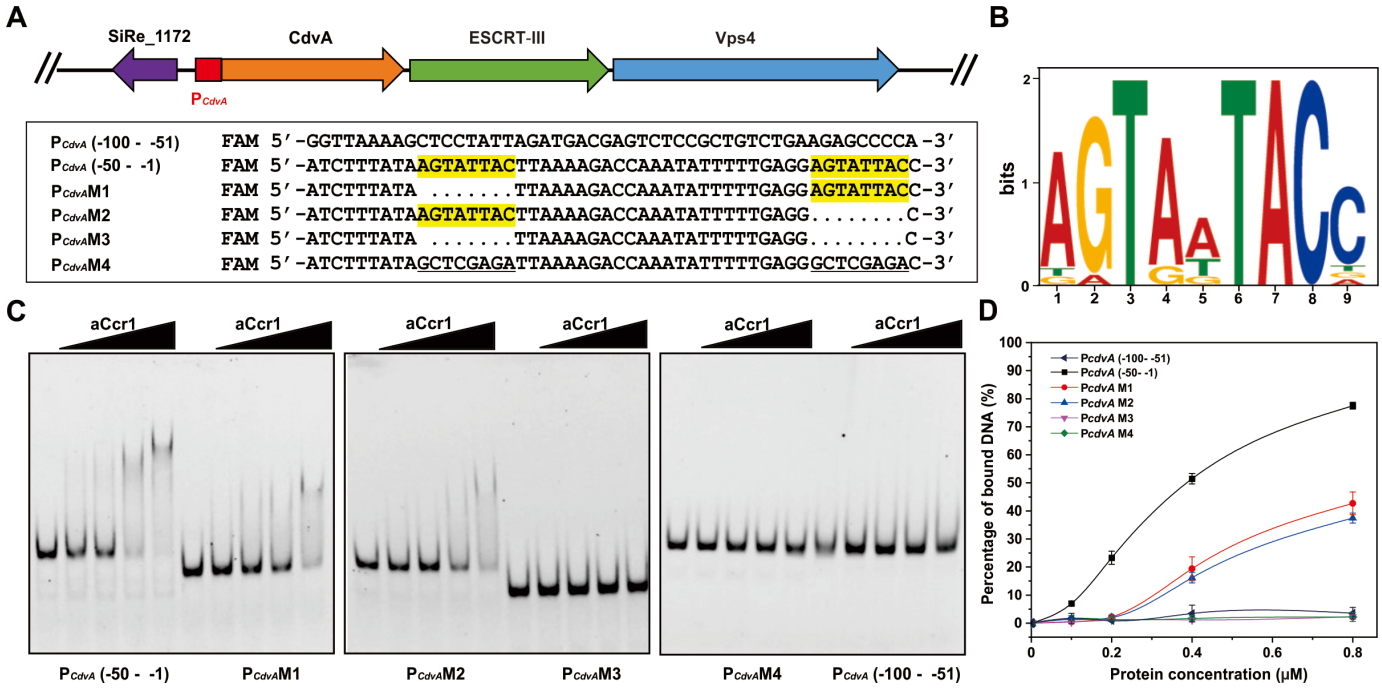


**Figure 4. aCcr1 binds to the promoter of *cdvA* at the aCcr1-box motif.** (**A**) Schematic organization of Cdv genes and *cdvA* promoter in the genome of *S. islandicus* REY15A. The sequences of the upper region (-100 - -51), lower region (-50 - -1) and its variant mutants used in the EMSA analysis are listed. The aCcr1-box motif is highlighted in yellow. Dots and the underlined indicate truncated and substitutive sequences, respectively. The oligonucleotides are labelled with FAM fluorescence at the 5' -ends for EMSA. (**B**) A conserved motif (designated as aCcr1-box) identified in the promoters of the highly repressed genes due to aCcr1 over-expression. A total of 15 promoter sequences (-60 - -1) of the down-regulated (>4 folds) genes plus promoter of *cdvA* from *Sulfolobus acidocaldarious* were used as the input for De Novo motif discovery by MEME server with the default setting. The height of the letter indicates the relative similarity to that of consensus one. (**C**) EMSA of aCcr1 binding to different regions of the promoter of *cdvA* and its mutants. The 5' FAM-labelled and corresponding complementary nucleotide sequences are listed in Table S2. The labelled oligonucleotides were annealed with the respective complementary strands as described in the Materials and Methods for the EMSA assay. The reaction was performed at 37C° for 30 min and analysed on a 10% native PAGE (see "Materials and Methods"). Each reaction contained 2 nM of the FAM-labelled probe and 0, 0.1, 0.2, 0.4, or 0.8 μM aCcr1 protein. (**D**) Quantification of the results in (C). The values were obtained from three independent experiments. Error bars indicate standard deviation.

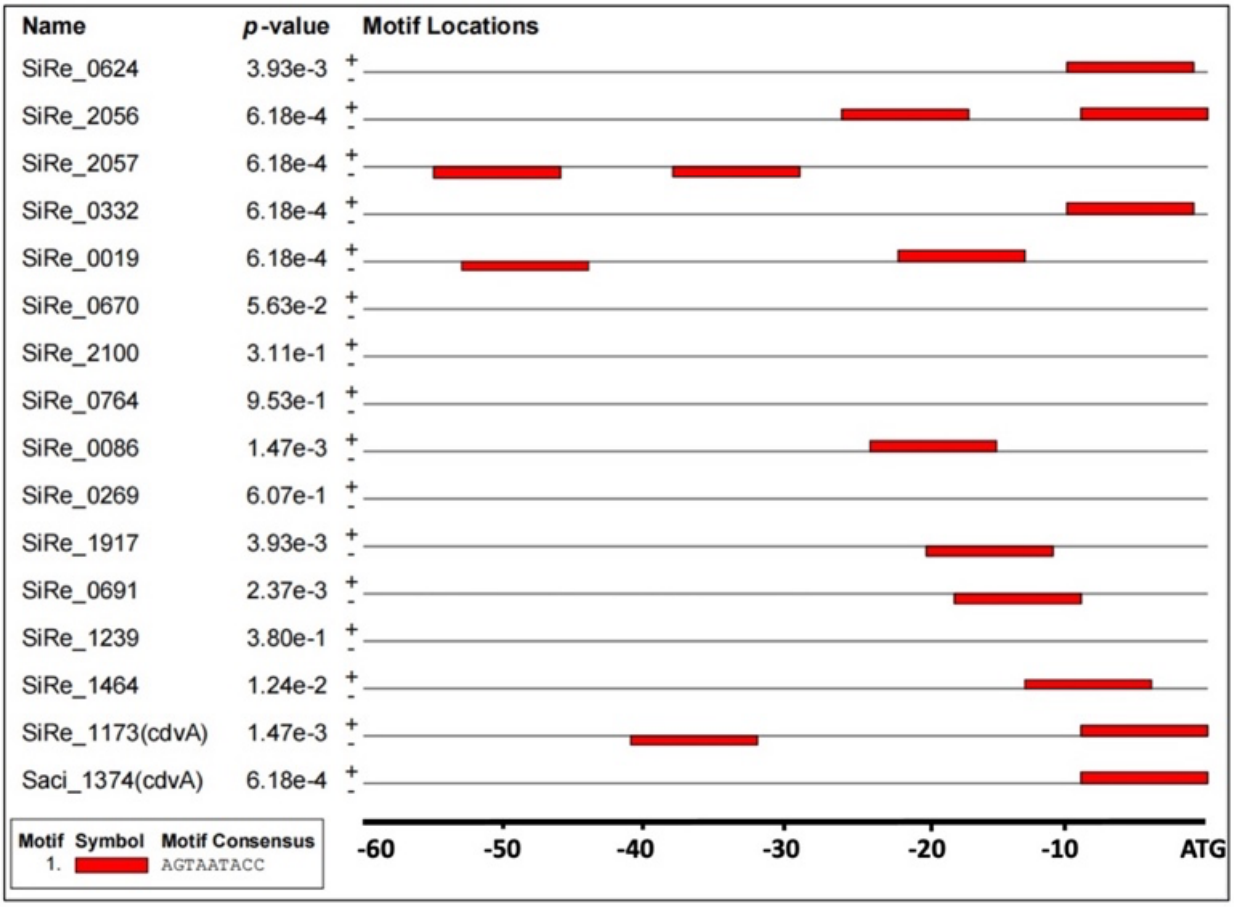


**Figure 5. Distribution of aCcr1-box in the highly repressed gene promoters.** "+" and "–" represent coding and non-coding strands, respectively.

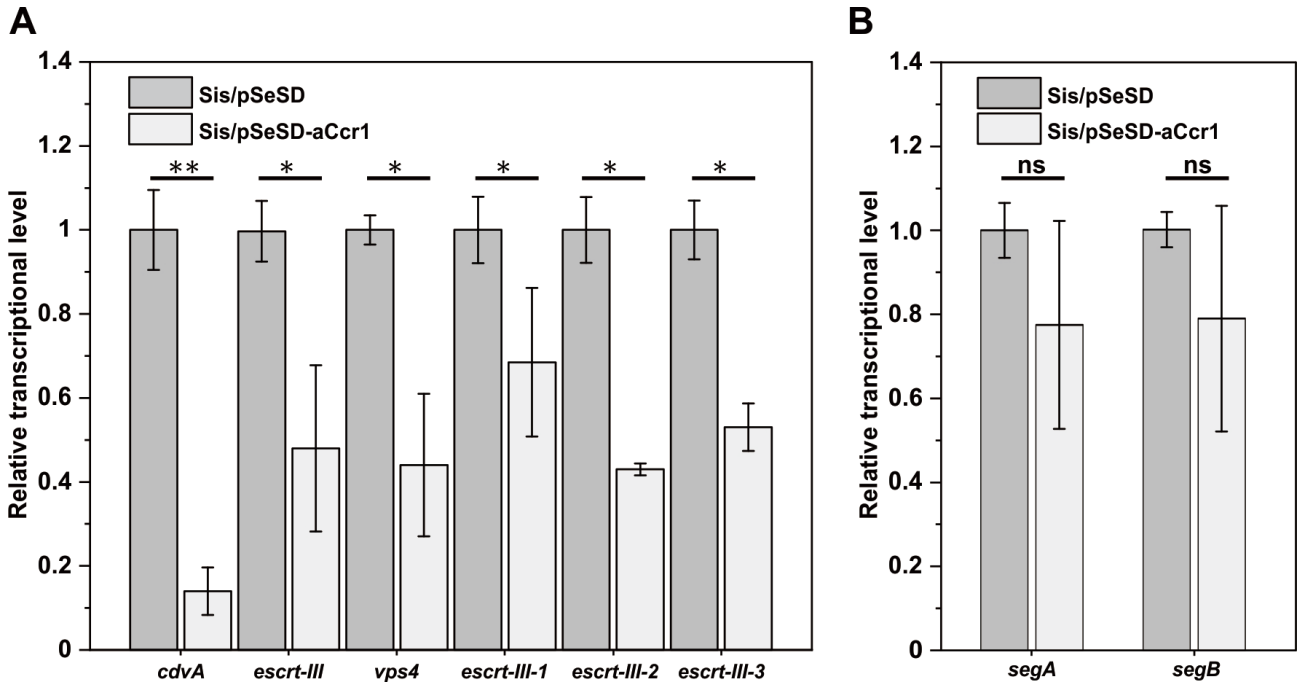


**Figure 6. The expression of cell division genes is down regulated and that of the chromosome segregation genes is unchanged in the aCcr1 over-expression cells.** Quantitative PCR (qPCR) analysis of the expression of cell division (**A**) and chromosome segregation genes (**B**) in aCcr1 over-expression cell in comparison with E233S cell carrying the empty vector (Sis/pSeSD). Cell cultures were sampled and analysed after 12 hours of arabinose induction. The 16S rRNA was used as the reference. The transcription levels of the target genes in the control strain (Sis/pSeSD) were defined as 1 (grey). *, P value<0.05; **, P value<0.01; ns, not significant. Error bars represent standard deviation from three independent repeats.

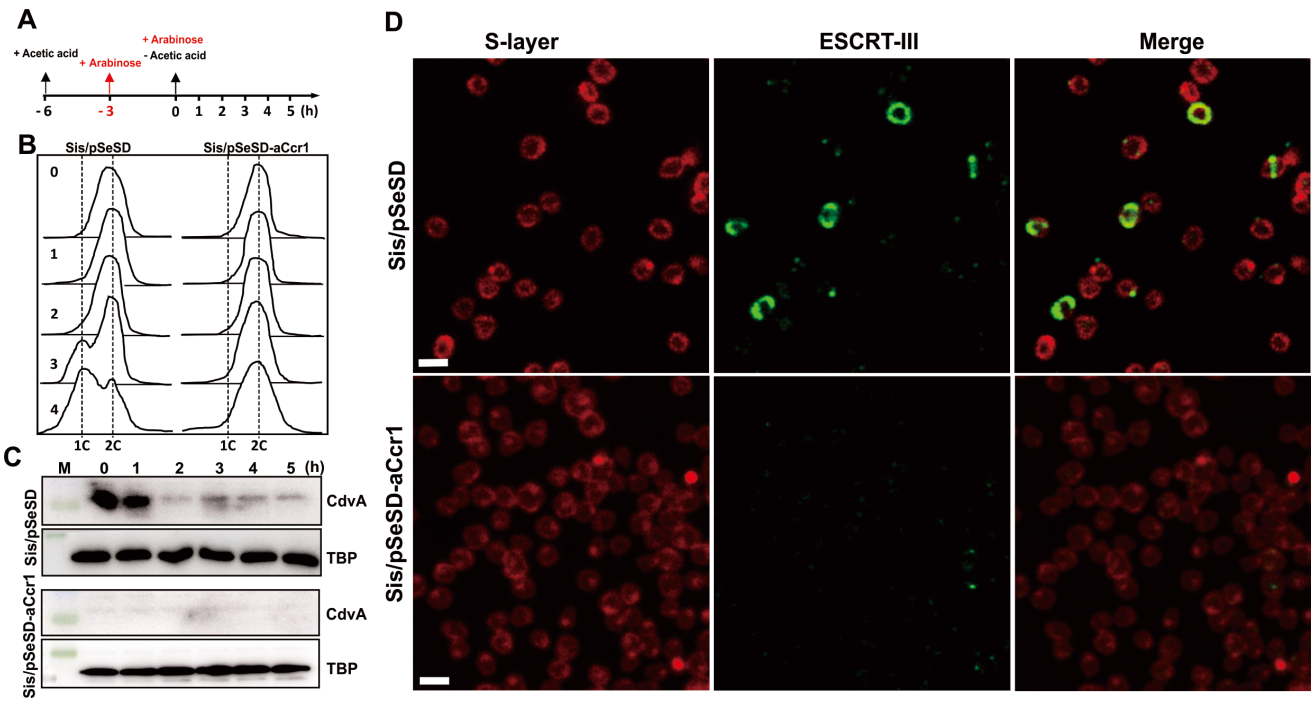


**Figure 7. Over-expression of aCcr1 stalls cell division and impairs the ESCRT-III contractile ring formation.** (**A**) Schematic showing the cell synchronization and induction of aCcr1 over-expression with arabinose (0.2%). Time for acetic acid treatment and arabinose induction are indicated. E233S containing the empty plasmid (Sis/pSeSD) was used as a control. (**B**) Flow cytometry profiles of DNA content distribution of cells 0-4 hrs after acetic acid removal. (**C**) Western blotting using anti-CdvA antibody in strain Sis/pSeSD-aCcr1 and the control at 0-5 hrs after acetic acid removal. TBP (TATA-box binding protein) was used as a loading control. The conditions for the Western blotting were as described in the Materials and Methods. Two gels and blots were used for each antibody with the same cell sample preparations and detection, except for CdvA, where 4 minutes was taken for exposure instead of 40 seconds. (**D**) Immuno-fluorescence microscopy showing the formation of contractile rings using the primary antibody against ESCRT-III (CdvB) and goat anti-rabbit secondary antibody Alexa Fluor® 488. The S-layer was stained with Concanavalin A, Alexa Fluor 647 Conjugate. Shown are representative images. M, molecular size marker.

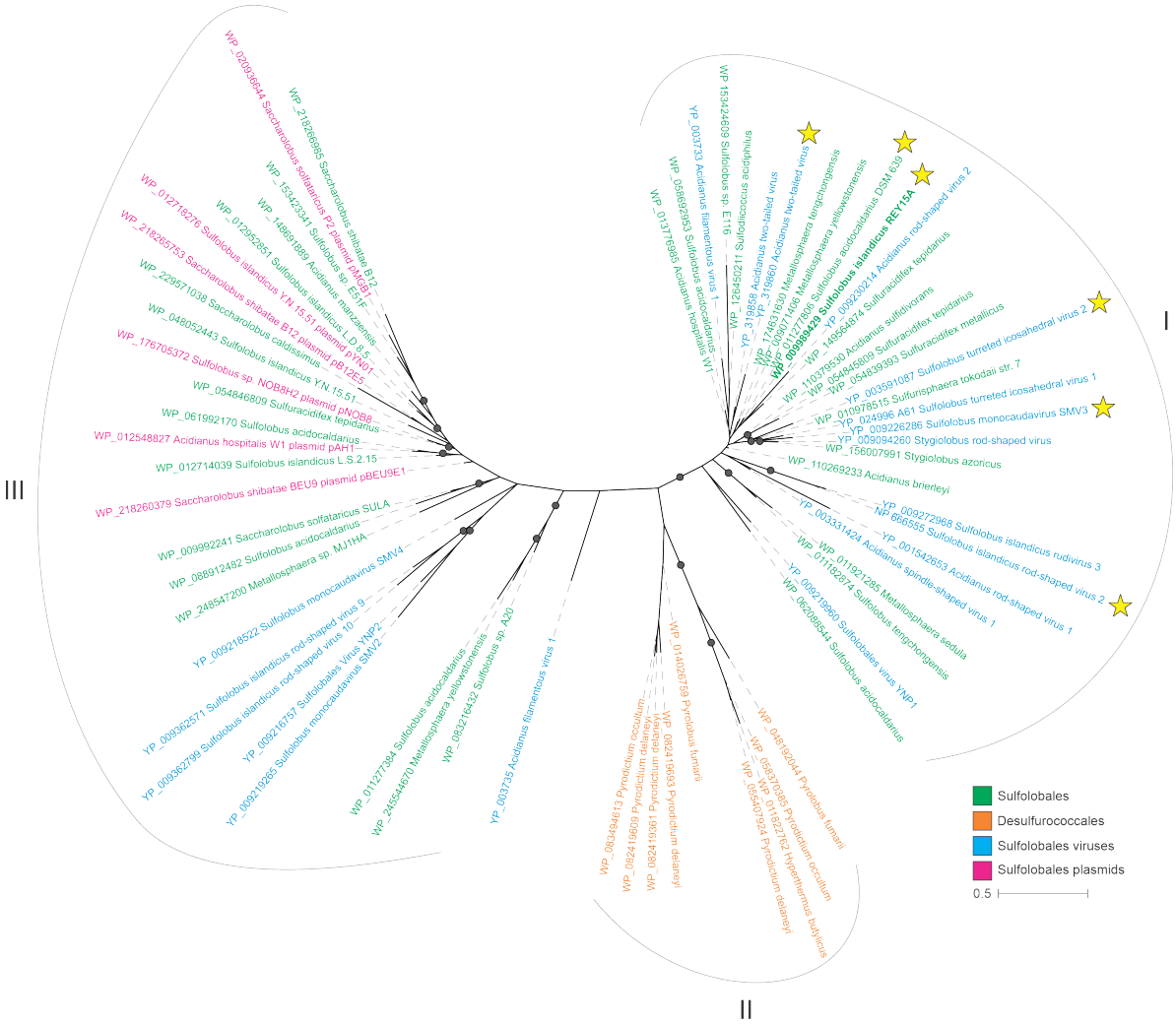


**Figure 8. aCcr1 homologs are widely distributed in Sulfolobales and Desulfurococcales as well as in the plasmids and viruses of Sulfolobales.** aCcr1 homologs were collected by PSI-BLAST. The collected sequences were then clustered using MMseq2. The sequences were aligned using MAFFT v7 and the resultant alignment trimmed using trimal. Phylogenetic analysis was performed using IQ-Tree and the branch support was assessed using SH-aLRT. The details of the analysis were listed in the Materials and Methods. The aCcr1 homologs investigated in this study were indicated with the yellow stars.

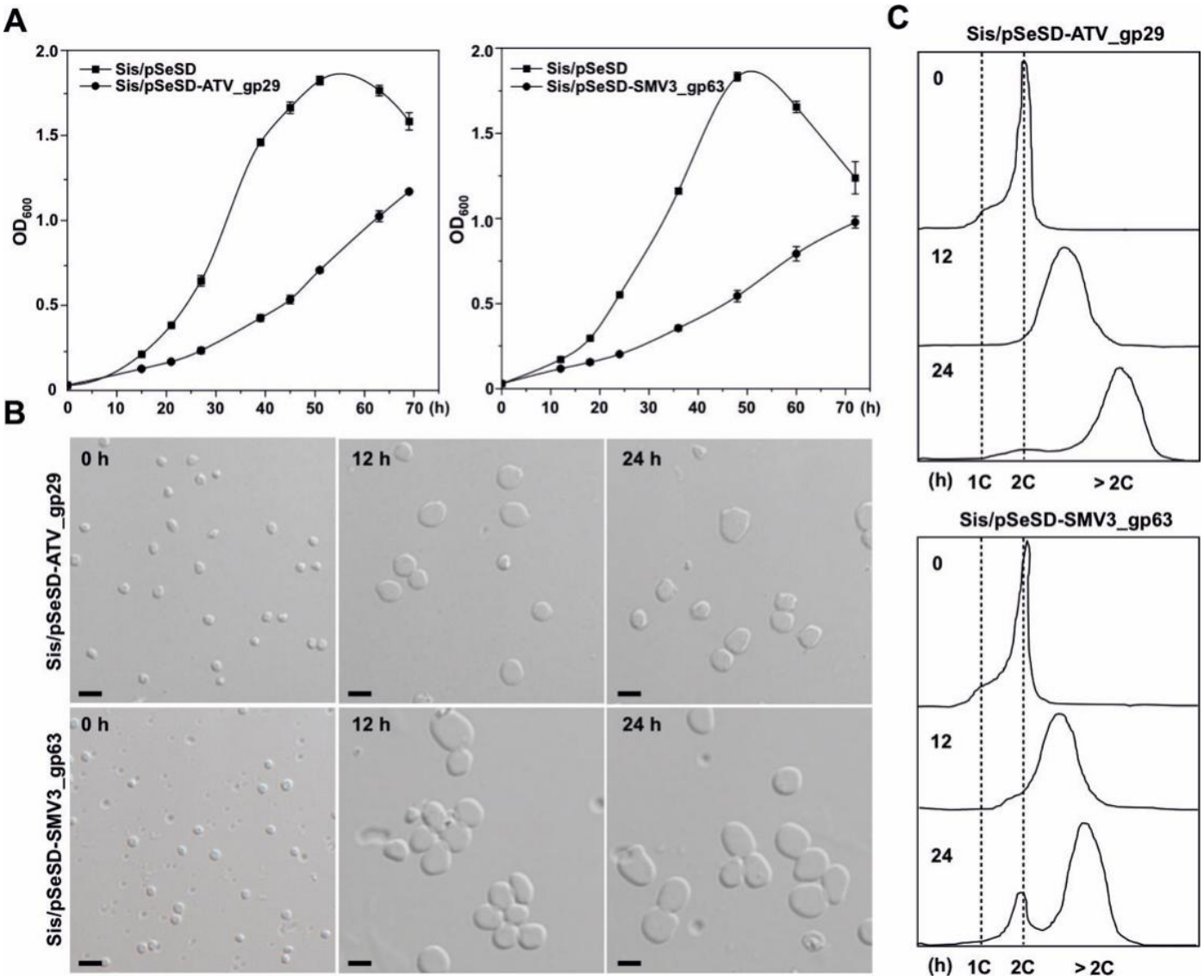


**Figure 9. Cells with over-expression of the aCcr1 homologs, ATV_gp29 from *Acidianus* Two-tailed Virus and SM3_gp63 from *Sulfolobus* monocadauvirus 3 have similar phenotype as those with over-expression of SisCcr1.** (**A**) Growth curves of cells Sis/pSeSD-ATV_gp29 and Sis/pSeSD-SMV3_gp63 cultured in induction medium ATV. The cells were inoculated into 30 ml medium to a final estimated $OD_{600}$ of 0.03 and the growth was monitored using spectrometer. Each value was based on data from three independent repeats. Cell harboring the empty plasmid pSeSD was used as a control. (**B**) Phase contrast microscopy and (**C**) flow cytometry of cells over-expressing ATV_gp29 and SMV3_gp63. Cells cultured in medium ATV were taken at different time and observed under an inverted fluorescence microscope for DNA content using an ImageStreamX MarkII Quantitative imaging analysis flow cytometry (Merck Millipore, Germany). Scale bars: 2 μm.

**Table 1. Summary of genes with >4 fold down-regulated at mRNA levels in the aCcr1 over-expression strain based on comparative transcriptomic analysis***

| Gene identity | Protein function | Sis/pSeSD-aCcr1 vs Sis/pSeSD log2 Fold Change |
|---|---|---|
| SiRe_0624 | Blue (type 1) copper domain-containing protein | -3.458533126 |
| SiRe_0623 | Uncharacterized membrane protein | -3.261849277 |
| SiRe_0670 | Zinc finger SWIM domain-containing protein | -3.153753639 |
| SiRe_2056 | Serine/threonine protein kinase | -3.077324891 |
| SiRe_0332 | Cellulase (endo 1,4 beta glucanase), putative (CelB) | -2.944384326 |
| SiRe_0764 | CRISPR-associated, Csa3a | -2.922021684 |
| SiRe_2100 | SedA, Membrane protein involved in DNA uptake | -2.918474234 |
| SiRe_0019 | Queuine/archaeosine tRNA-ribosyltransferase | -2.906286786 |
| SiRe_0086 | ATPase, predicted component of phage defense system | -2.817790738 |
| SiRe_0018 | Queuine tRNA-ribosyltransferase related protein | -2.789165379 |
| **SiRe_1173** | **Cell division protein CdvA** | **-2.669806305** |
| SiRe_2057 | Uncharacterized membrane protein | -2.249728764 |
| SiRe_1917 | AIR synthase related protein | -2.226944702 |
| SiRe_0691 | Thermopsin-like protease | -2.224399679 |
| SiRe_1464 | Uncharacterized protein | -2.069938647 |
| SiRe_0269 | Uncharacterized protein | -2.045724686 |
| SiRe_1239 | Zn-dependent alcohol dehydrogenase | -2.030511419 |

* The cell division protein CdvA is shown in bold.

**Table 2. Distribution of aCcr1-box in the promoter of highly down-regulated genes in the aCcr1 overexpressing strain and CdvA homologs from other archaeal species***

| Gene identity | Promoter Sequences (-50 - +3) |
|---|---|
| SiRe_0624 | TAGGTTCCATTAATCACAAAATTTTTTAACCTATGTACTAAGTAATACGTATG |
| SiRe_2056 | ATACACATTGGGCTAAATATTTTAAGTGTTACCAGTAAAATAGTAATACCATG |
| SiRe_0332 | AATAGCATTAACCTACTAATTTTTTAAAATTGCCAAAGTAAGTAATACCTATG |
| SiRe_0018 | ATTATTATAAATGAAGTTATAACCCGATAGTAATACCAATACCAGGAAAAATG |
| SiRe_0086 | GCTAACGATTATATTTTATTCTGCTAAGTATTACCGTAGAGTGATCTGTAGTG |
| SiRe_0269 | GAAAATACTTTCGTGAATCTCAGTAGTGTTTTTTAAGTAAAATTTCTGATATG |
| SiRe_1917 | AATCGTGTGATGGGAAAAATATATTATAATGGTATTACATTTTGCGTTTAATG |
| SiRe_0691 | AGCATTACTATAACAATATTTAAATATAACATGGTACTACCCTTTTACCCATG |
| SiRe_1464 | CCATAAACCTTAGGATAAACGTTATAACTAGCTAATAAGTAGTACACGTAATG |
| SiRe_1173 (CdvA) | ATCTTTATAAGTATTACTTAAAAGACCAAATATTTTTGAGGAGTATTACCATG |
| Saci_1374 (CdvA) | AATTCTTATAAATATAATCATCATAGCTGATAACTTTGAGGAGTAATACCATG |
| Ahos_1333 (CdvA) | TAACCTTTTTAAATATTTTATCTCAACATGTAACTTTGAGGAGTATTACCATG |
| Mcup_0558 (CdvA) | TCCTTTTAAATCGTTCCAAACTTAACTTGTATTTTTGAGGAGTATTACCTATG |
| IC006_1093 (CdvA) | ATCCTTTTAAAGCGAAATACTTAACCTCTAGCTTTTGAGGAGTAATACCTATG |
| D1868_04805 (CdvA) | AATCCTTTTAAATAAATCATACTCAGCTGATAATTTTGAGGAGTAATACCATG |

* The aCcr1 box sequences are underlined and highlighted in yellow (sense strand) or green (antisense strand). The translation start codes are shown in red. SiRe_0019, SiRe_0623, and SiRe_2057 are not listed because they are in the same operon with of SiRe_0018 and SiRe_0624, respectively, or shares a bidirectional promoter with SiRe_2056.